International Journal of Computational and Experimental Science and ENgineering (IJCESEN)

Vol. 11-No.3 (2025) pp. 4277-4284
http://www.ijcesen.com

ISSN: 2149-9144

Research Article

Homogenized failure model of corrugated sandwich panels under tension

Viet Dung Luong*

Faculty of Mechanical Engineering, Thai Nguyen University of Technology, Vietnam
*** Corresponding Author Email:** luongvietdung@tnut.edu.vn- **ORCID**: 0000-0002-3093-837X

Article Info:

DOI: 10.22399/ijcesen.2969
Received : 23 April 2025
Accepted : 10 June 2025

Keywords

Finite Element Simulation
Homogenization
Subroutine
Cardboard

Abstract:

Corrugated core sandwich panels are widely used due to their high strength-to-weight ratio and superior energy absorption. This paper presents a finite element homogenization model to predict the mechanical failure behavior of corrugated core sandwich panels under tension. The homogenization method simplifies the complex core geometry while preserving the mechanical properties of the structure. A homogeneous 2D plate replaces the 3D model of the panel with isotropic properties. The mechanical behavior model of Chow and Wang is used to describe the response of each material layer. The homogenization process is performed through local integration over the thickness of the layers. The model is implemented in Abaqus software through the UGENS user subroutine. The results from the model are compared with full 3D simulations, demonstrating the computational efficiency, model-building time, and accuracy of the proposed method.

1. Introduction

Corrugated sandwich panels are widely used in industries such as aerospace and construction due to their lightweight properties and superior load-bearing capacity. These structures have complex failure mechanisms under various loading conditions, making their failure prediction an essential issue in design optimization. Understanding the mechanical behavior of corrugated sandwich panels under tensile forces is important to ensure reliability and safety in practical applications. To date, many studies on sandwich panels have been published [1–11]. In these studies, experiments are often used to determine the mechanical properties of sandwich panels [2], thereby providing analysis and evaluation to support the design process. However, these experiments are not always performed due to the high cost. Therefore, the approach in many studies is to use numerical simulation to model the experiments [9] to reduce costs in the product design process. For example, Marc R. Schultz et al [12] studied the design of corrugated core sandwich panels. The axial compression performance of the panels was evaluated using experiments and finite element analysis (FEA). Detailed finite element models were developed to represent all components of the corrugated core structure, and geometric nonlinear analyses were performed to predict both buckling and material failure. The experimental data agreed with the analysis in both cases of local buckling and material failure. A theoretical analysis employing the energy method is conducted through experimentation and simulation to predict the mechanical behavior of corrugated aluminum core sandwich panels under significant deformation [13].

The above analysis shows that the use of finite element models brings many benefits to engineering design and structural analysis, such as: FEM allows detailed analysis of stress, deformation, temperature and other physical phenomena; Reducing the number of experimental tests, thereby saving materials and testing time; Allows testing of multiple design options without the need to fabricate physical prototypes; Can analyze nonlinear phenomena such as plastic deformation, material failure, contact between parts; Easily perform geometry and material optimization problems to achieve the highest performance; Predicts weaknesses in design, avoiding manufacturing errors or premature failures during operation; Provides information to improve designs before actual production. Therefore, FEM has become an indispensable tool in modern

engineering, helping to improve the quality and performance of products right from the design stage, especially for complex structures such as sandwich panels. However, the use of FEM models for calculation is facing the problem of reducing calculation time. To solve this problem, the homogenization method has been used.

Most developed and published homogeneous models focus on corrugated sandwich panel structures [14–26]. Guo et al [16] study has built an elastic homogenization model for corrugated core cardboard panels. The model has accurately described the panel behavior as well as significantly reduced the model's calculation time. An equivalent elastic-plastic model is presented in Luong's study to study the mechanical behavior of corrugated cardboard structures under varying loads [25] . Up to now, homogeneous models have stopped at studying elastic and plastic behavior. There is no unified model that studies damage behavior. This study develops a unified model to investigate the damage behavior of sandwich panels subjected to tensile loading. The parameters in the Chow-Wang behavior model for paper layers are determined by integrating numerical and experimental approaches. The homogenization model is constructed based on the integration over the thickness of each layer, providing the local equivalent strain. The proposed homogenization model is implemented in the ABAQUS finite element software using the UGENS subroutine. The results obtained from the proposed model are compared with those from full 3D simulations under tensile loading conditions.

2. Homogenization model

Homogenization modelling is the process of using mathematical and theoretical methods to simulate physical systems with heterogeneous structures. The goal of homogenization is to find average quantities that represent the overall mechanical behavior, thereby allowing accurate prediction of material properties without the need for detailed microscopic analysis.

2.1 The mechanical behavior of the model

In this study, the Chow and Wang model [27] is used to describe the mechanical behavior of each layer. Based on the anisotropic theory of damage mechanics, a damage characteristic tensor is constructed and developed to describe the anisotropic damage growth. The failure properties of materials undergoing large plastic deformation and anisotropic plasticity have been developed in the main directions through the constitutive equations. The deformation of damaged materials, according to the von Mises strain criterion, is defined:

$$F_p(\sigma, D, R) = F_p(\tilde{\sigma}, R) = \tilde{\sigma}_p - \{R_0 + R(p)\} = 0 \quad (1)$$

where R_0 is the initial strain hardening threshold, R(p) is the strain hardening increase threshold, and is the effective equivalent plastic stress, with.

$$\tilde{\sigma}_p = \left\{\frac{1}{2}\tilde{\sigma}^T : \underline{H} : \tilde{\sigma}\right\}^{1/2} = \left\{\frac{1}{2}\sigma^T : \underline{H} : \sigma\right\}^{1/2} \quad (2)$$

Where

$$\underline{H} = \underline{M}^T(D) : \underline{H} : \underline{M}(D) \quad (3)$$

$$[H] = \begin{bmatrix} G+H & -H & -G & 0 & 0 & 0 \\ & H+F & -F & 0 & 0 & 0 \\ & & F+G & 0 & 0 & 0 \\ S & & & 2L & 0 & 0 \\ & & & & 2M & 0 \\ & & & & & 2N \end{bmatrix} \quad (4)$$

where F, G, H, L, M, and N are parameters characterizing the current state of plastic anisotropy in Hill's behavior model. The increase in the strain hardening threshold is represented by Equation (5)

$$R(p) = Kp^n \quad (5)$$

where p is the accumulated plastic strain, and K and n are material constants. Constitutive equations of plastic behavior and material failure

$$\dot{\varepsilon}^p = \lambda_p \frac{\partial F_p}{\partial \sigma} = \frac{\lambda_p}{2\tilde{\sigma}_p} = \underline{\tilde{H}} : \sigma \quad (6)$$

$$\dot{p} = \lambda_p \frac{\partial F_F}{\partial(-R)} = \lambda_p \quad (7)$$

$$\lambda_p = \begin{cases} \dfrac{\dfrac{\partial F_p}{\partial \sigma} : \dot{\sigma} + \dfrac{\partial F_p}{\partial \sigma} : \dot{D}}{\left(\dfrac{\partial F_p}{\partial R}\right)^2 \left(\dfrac{\partial R}{\partial \dot{p}}\right)} > 0 \\ \text{if } F_p = 0 \text{ and } \dfrac{\partial F_p}{\partial \sigma} : \dot{\sigma} \dfrac{\partial F_p}{\partial D} : \dot{D} > 0 \end{cases} \quad (8)$$

$$\dot{p} = 2\left(\frac{1}{2}\dot{\varepsilon}^p : \tilde{\underline{H}}^{-1} : \dot{\varepsilon}^p\right)^{1/2} = 2\left[\frac{1}{2}\left\{\dot{\varepsilon}^p\right\}^T \left[\tilde{\underline{H}}\right]^{-1} \left\{\dot{\varepsilon}^p\right\}\right]^{1/2}$$

The following formula calculates the cumulative plastic strain rate

$$\dot{p} = 2\left(\frac{1}{2}\dot{\varepsilon}^p : \tilde{\underline{H}}^{-1} : \dot{\varepsilon}^p\right)^{1/2} = 2\left[\frac{1}{2}\left\{\dot{\varepsilon}^p\right\}^T \left[\tilde{\underline{H}}\right]^{-1} \left\{\dot{\varepsilon}^p\right\}\right]^{1/2} \quad (9)$$

where $\left[\tilde{H}\right]^{-1}$ is the generalized inverse of the singular matrix $\left[\tilde{H}\right]$ [28]. A damage tensor is constructed to describe the development of damage. The damage criteria are calculated as follows

$$F_d = Y_{II}^{1/2} - (B_0 + B(\beta)) = 0 \quad (10)$$

where β is overall damage, B_0 is initial damage threshold, and B(β) is increment of damage threshold depending on β, where

$$Y_{II} = \frac{1}{2} Y^T : \underline{J} : Y \tag{11}$$

where J is a fourth-order symmetry tensor, and Y is called the damage strain energy release rate

$$Y = -\varepsilon^e : (\underline{M}^{-1} : \frac{\partial \underline{M}}{\partial D} : \tilde{\underline{C}})^s : \varepsilon^e = -\sigma : (\tilde{\underline{C}}^{-1} : \underline{M}^{-1} : \frac{\partial \underline{M}}{\partial D})^s : \sigma \tag{12}$$

Finally, F_d is calculated by the formula

$$F_d = \tilde{\sigma}_d - [B_0 + B(\beta)] = 0 \tag{13}$$

$\tilde{\sigma}_d$ is effective damage equivalent stress

$$\tilde{\sigma}_d = (\frac{1}{2}\tilde{\sigma}^T : \underline{J} : \tilde{\sigma})^{1/2} = (\frac{1}{2}\sigma^T : \tilde{\underline{J}} : \sigma)^{1/2} \tag{14}$$

$$\tilde{\underline{J}} = \underline{M}^T : \underline{J} : \underline{M} \tag{15}$$

$$\tilde{\sigma}_d = (\frac{1}{2}\tilde{\sigma}^T : \underline{J} : \tilde{\sigma})^{1/2} = (\frac{1}{2}\sigma^T : \tilde{\underline{J}} : \sigma)^{1/2} \tag{16}$$

$$\dot{D} = \lambda_d \frac{\partial F_d}{\partial \sigma} = \frac{\lambda_d}{2\tilde{\sigma}_d} \tilde{\underline{J}} : \sigma \tag{17}$$

$$\dot{\beta} = \lambda_d \frac{\partial F_d}{\partial (-B)} = \lambda_d \tag{18}$$

$$\lambda_p = \begin{cases} \dfrac{\frac{\partial F_p}{\partial \sigma} : \dot{\sigma} + \frac{\partial F_p}{\partial \sigma} : \dot{D}}{\left(\frac{\partial F_p}{\partial B}\right)^2 \left(\frac{\partial B}{\partial \beta}\right)} > 0 \\ \end{cases} \tag{19}$$

$$if\ F_p = 0\ \ and\ \ \frac{\partial F_p}{\partial \sigma} : \dot{\sigma} \frac{\partial F_p}{\partial D} : \dot{D} > 0$$

$$if\ F_p < 0,\ or\ F_p = 0\ and\ \frac{\partial F_p}{\partial \sigma} : \dot{\sigma} \frac{\partial F_p}{\partial D} \dot{D} \le 0$$

Finally, the overall damage rate $\dot{\beta}$ is derived as

$$\dot{\beta} = 2(\frac{1}{2}\dot{\mathrm{D}} : \underline{\mathrm{J}}^{-1} : \dot{\mathrm{D}})^{1/2} \tag{20}$$

The parameters in the Chow-Wang behavior model will be calculated from experiments in the following section

$$F_d = Y_{II}^{1/2} - (B_0 + B(\beta)) = 0 \tag{21}$$

$$\dot{\beta} = 2(\frac{1}{2}\dot{\mathrm{D}} : \underline{\mathrm{J}}^{-1} : \dot{\mathrm{D}})^{1/2} \tag{22}$$

where p is overall damage, B_0 is initial damage threshold, and B(p) is increment of damage threshold depending on p and other parameters to be discussed later. The quadratic function Y was proposed to assume the form as

$$\mathrm{Y_{II}} = \frac{1}{2}\mathrm{Y^T} : \underline{\mathrm{J}} : \mathrm{Y} \tag{23}$$

Where J is the 4th order symmetry tensor, Y is

$$Y = -\varepsilon^e : (\underline{M}^{-1} : \frac{\partial \underline{M}}{\partial D} : \tilde{\underline{C}})^s : \varepsilon^e = -\sigma : (\tilde{\underline{C}}^{-1} : \underline{M}^{-1} : \frac{\partial \underline{M}}{\partial D})^s : \sigma$$

$$-Y_i = \frac{\sigma_i}{1-D_i} \frac{C_{ij}^{-1}}{(1-D_i)(1-D_j)} \sigma_j = \tilde{\sigma}_i \tilde{C}_{ij}^{-1} \sigma_j \tag{24}$$

$$\dot{D}_i = \frac{\dot{\beta}}{2Y_{II}^{1/2}} J_{ij}(-Y_j)$$

This model was implemented into the Abaqus software using the user subroutine VUMAT

2.2 Homogenization model

The homogenization method is based on laminated plate theory [29]. First, the elastic homogenization model is reconstructed and expanded to include plastic and damage behavior. The elastic-plastic homogenization model was developed in the studies by Luong et al [21]–[25]. Accordingly, the homogenization method is applied to a representative element for the sandwich panel structure with a corrugated core, as illustrated in Figure 1. The mechanical properties of the periodic unit cell will be used to model the 3D structure using an equivalent 2D plate. Accordingly, the relationship between the dimensional components is as follows:

$$h(x) = \frac{h_c}{2}\sin(\frac{2\pi x}{P})\ ;\ \theta(x) = \arctan(\frac{dh(x)}{dx}) \tag{25}$$

The matrices A_{ij}, B_{ij}, and D_{ij} representing the film stiffness, the combination of film and bending-torsion, and bending and torsional stiffness, respectively, are modified to suit the cardboard sheets

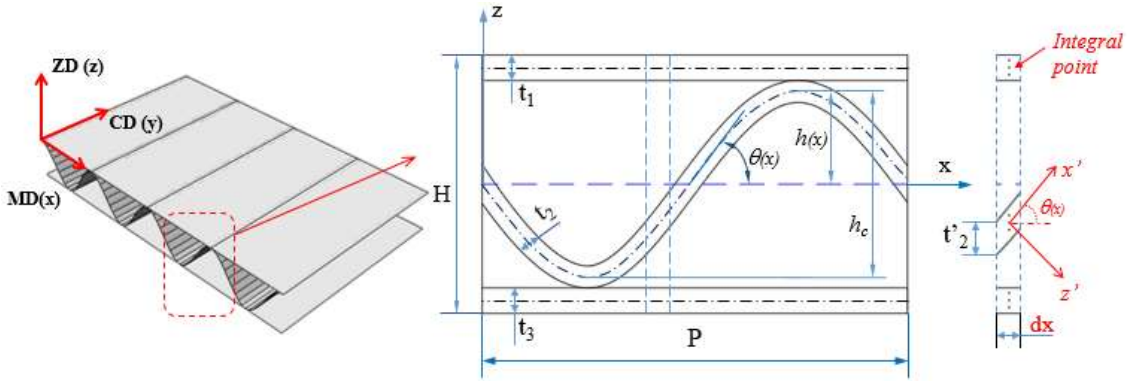

Figure 1. *Corrugated core sandwich panels and VER*

$$A_{ij} = \sum_{k=1}^{3} Q_{ij} t_k = Q_{ij}^{(1)} t_1 + Q_{ij}^{(2)}(\theta(x)) t_2^{'} + Q_{ij}^{(3)} t_3 \quad (26)$$

$$B_{ij} = \sum_{k=1}^{3} Q_{ij} z_k t_k = Q_{ij}^{(1)} z_1 t_1 + Q_{ij}^{(2)}(\theta(x)) z_2 t_2^{'} + Q_{ij}^{(3)} z_3 t_3 \quad (27)$$

$$D_{ij} = \sum_{k=1}^{3} Q_{ij}(z_k^2 t_k + \frac{1}{12} t_k^3)$$
$$= Q_{ij}^{(1)}(z_1^2 t_1 + \frac{1}{12} t_1^3) + Q_{ij}^{(2)}(z_2^2 t_2^{'} + \frac{1}{12} t_2^{'3}) + Q_{ij}^{(3)}(z_3^2 t_3 + \frac{1}{12} t_3^3) \quad (28)$$

$$F_{ij} = \frac{5}{6}(C_{ij}^{(1)} t_1 + C_{ij}^{(2)}(\theta(x)) t_2^{'} + C_{ij}^{(3)} t_3) \quad (29)$$

$$\text{with } t_2^{'} = \frac{t_2}{\cos\theta(x)}$$

The average stiffness of all slices in the sinusoidal period P, in the MD direction, is calculated according to the formulas:

$$A_{ij}^{H} = \frac{1}{P}\int_0^P A_{ij}(x)dx \; ; \; B_{ij}^{H} = \frac{1}{P}\int_0^P B_{ij}(x)dx$$
$$D_{ij}^{H} = \frac{1}{P}\int_0^P D_{ij}(x)dx \; ; \; F_{ij}^{H} = \frac{1}{P}\int_0^P F_{ij}(x)dx \quad (30)$$

The algorithms for the Chow and Wang behavior model are applied at each corrugated cardboard layer, to calculate the stress state and the matrices in the local coordinate system using three integration points for each layer. Note that the local coordinate system of the core layer is defined by the angle $\theta(x)$. Accordingly, the stress state and the matrices are updated after each increment using the variables in the UGENS subroutine. Finally, the matrices [A], [B], and [D] will be replaced by their corresponding matrices in the case of plastic-damage behaviour.

3. Results and Discussions

To validate the proposed model, in this section, we will perform tensile simulations for the 3D model of the cardboard and the 2D homogenization model. First, the inverse identification procedure is applied to determine the material parameters in the Chow and Wang behavior model. These parameters will then be used to input into the simulation model to perform numerical simulations.

3.1 Determination of material parameters

This section applies the proposed homogenization model to corrugated cardboard structures. Cardboard consists of multiple layers of paper. The manufacturing process produces three characteristic directions: the machine direction (MD), the cross direction (CD), and the thickness direction (ZD). Each paper layer exhibits a rather complex, anisotropic, and nonlinear behavior. The stiffness in the MD direction is 2 to 4 times greater than in the CD direction, but the deformation in the CD direction is larger[19], [30].

This model can be extended to other types of sandwich corrugated core structures by using appropriate behavior rules. To evaluate the proposed model, the material parameters in the Chow and Wang model need to be determined for the layers. Figure 2 and Table 1 show the studied carton's structural parameters.

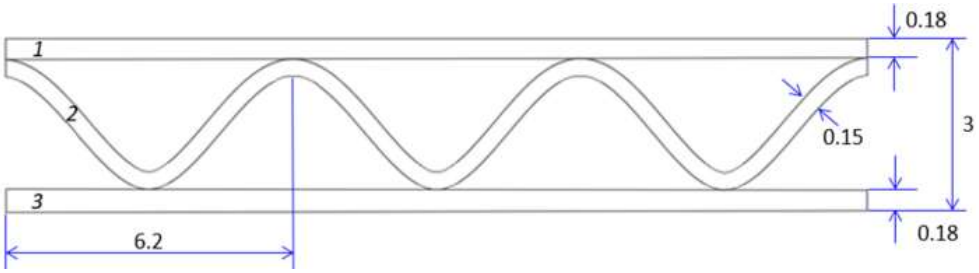

***Figure 2**. Dimensions of corrugated cardboard constituents*

***Table 1**. Cardboard plate properties*

	Grammage (g/mm²)	Thickness (mm)
Liner	140	0.18±0.004
Fluting	113	0.15±0.008
Liner	140	0.18±0.004

The inverse determination method was used to determine the material parameters [31]. Accordingly, tensile tests of samples in MD, CD, and 45^0 directions were performed; the results are shown in Figure 3 and Figure 4. At the same time, finite element simulations of the tensile tests were also performed. Then, the quadratic difference between the numerical and experimental results is evaluated through the objective function (31).

$$F_{obj} = \frac{1}{N}\sum_{i=1}^{N}\left(F_{num}(U_{num}) - F_{\exp}(U_{\exp})\right)^2 \quad (31)$$

Where $F_{num}(U_{num})$ and $F_{num}(U_{num})$ are the model force and experimental force with corresponding deformation, respectively, N is the number of the data set.

The three-directional tensile tests (MD, CD, and 45^0) were simulated using the finite element model, and the numerical results were compared with the experimental data. Figure 5 and Figure 6 presents a comparison between the experimental and numerical results obtained for the flat layers according to the Chow and Wang model. It is evident that the constitutive model accurately predicts the material's mechanical behavior in three directions. The material parameters determined in the Chow-Wang model for each layer are summarized in Table 2 and Table 3.

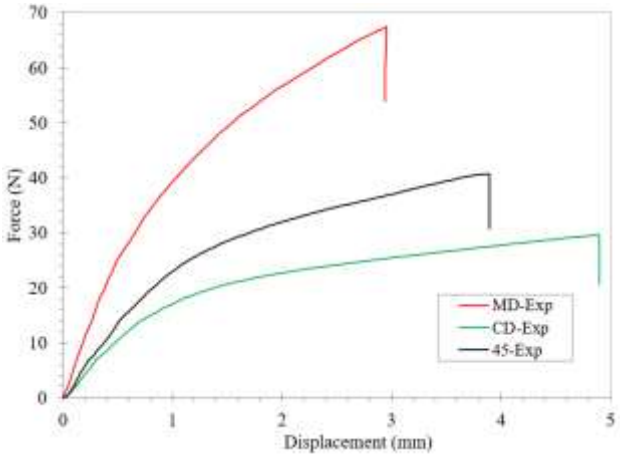

Figure 3. *Force vs displacement relationship of paper specimens 1 and 3*

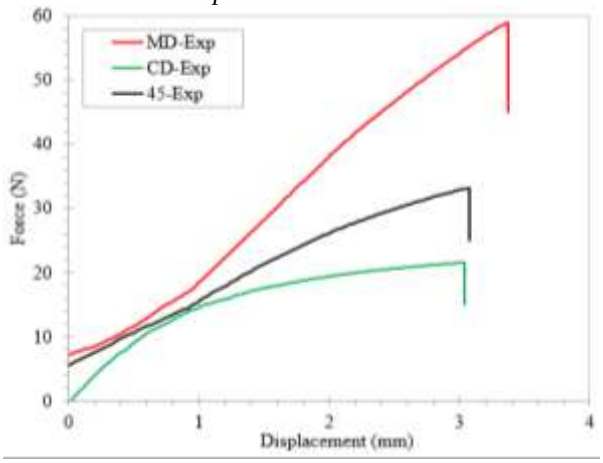

Figure 4. *Force vs displacement relationship of paper specimen 2*

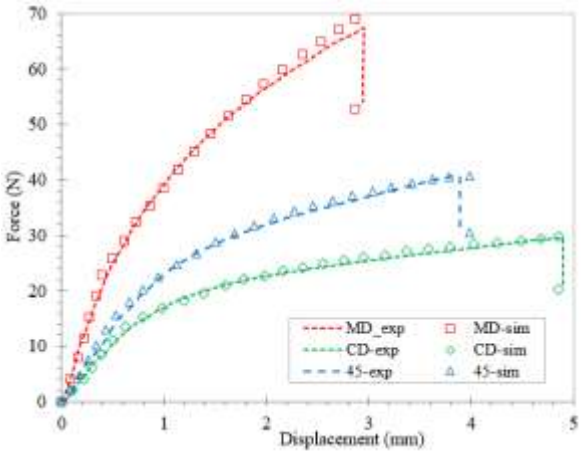

Figure 5. *Experimental and numerical results of tensile test for specimens 1 and 3*

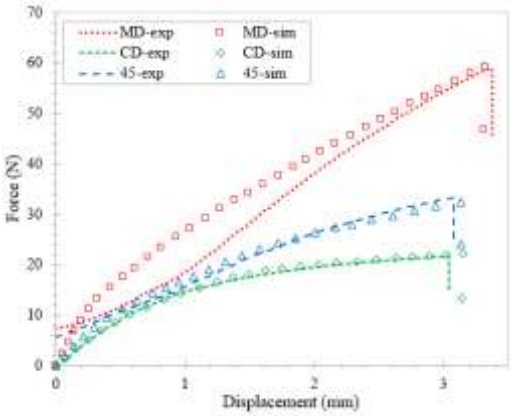

Figure 6. *Experimental and numerical results of tensile test for specimen*

3.2 Simulation of tensile test

To validate the proposed model, numerical simulations for the tensile cardboard plate were performed in MD and CD directions using the proposed 2D homogenization model and the full 3D model. The dimensions of the plate are shown in Figure 7. Accordingly, one end of the sample is clamped tightly, and traction is applied to the other end. The 3D structure and the 2D homogenization plate were meshed using reduced rectangular integral shell (S4R) elements with a mesh size of 0.5 mm. Figure 8 compares the simulation results of the 3D carton board structure and the 2D homogeneous board. The presented results show a very good agreement between the full 3D and the homogeneous 2D FEM solutions. The failure limit of the two tensile models is close to each other. The CPU times of the homogeneous model are 5.5 times faster than the full 3D model in the MD direction and 5.67 times faster in the CD direction (Figure 9). The results show that the proposed model is reliable in the case of corrugated core sandwich panels under tension

Table 2. *Material parameters in Chow Wang behavior model for paper layer 2*

E_1 (MPa)	E_2 (MPa)	ν_{12}	G_{12} (MPa)	R_{11}	R_{22}
3034	1454	0.05	705.4	1	0.41
R_{12}	d_{sw}	μ	$dB/d\beta$	B_0	d_{cr1}
0.55	1	1	389	10.7	0.3
d_{cr2}	β_{cr}	ε_0	K(MPa)	n	
0.37	0.8	0.027	527	0.21	

Table 3. *Material parameters in Chow Wang behavior model for layer 1 and 3.*

E_1 (MPa)	E_2 (MPa)	ν_{12}	G_{12} (MPa)	R_{11}	R_{22}
3089	1501.5	0.23	736.9	1	0.44
R_{12}	d_{sw}	μ	$dB/d\beta$	B_0	d_{cr1}
0.55	1	1	544.4	12.76	0.35

d_{cr2}	β_{cr}	ε_0	K(MPa)	n	
0.38	0.95	0.064	643	0.25	

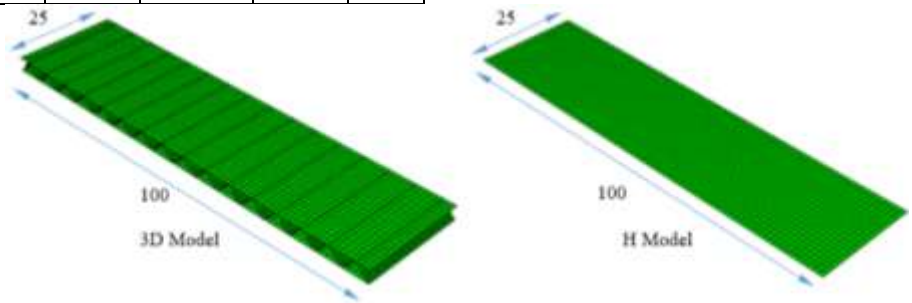

Figure 7. *3D model and H model of corrugated core board*

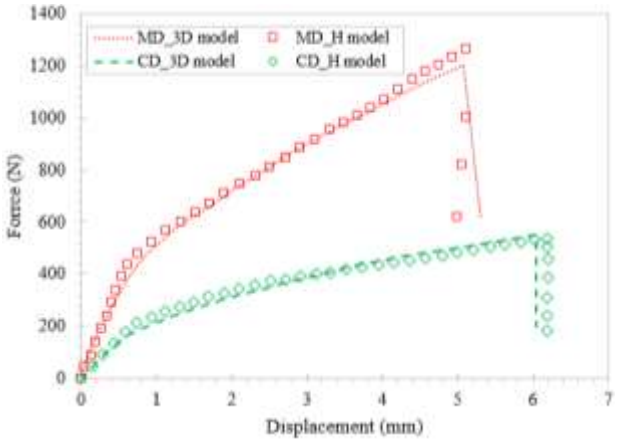

Figure 8. *Comparison of the behavior of homogeneous and 3D panel*

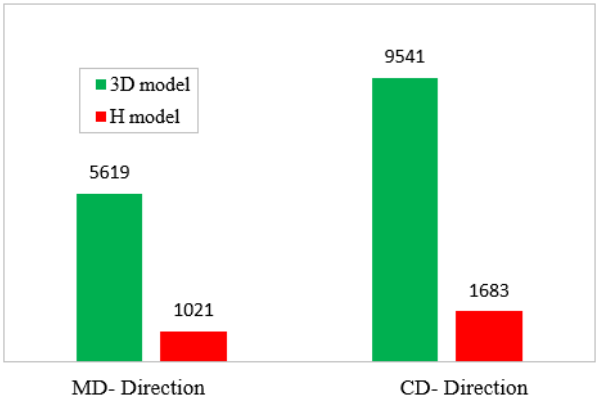

Figure 9. *Comparison of CPU times (in seconds)*

4. Conclusions

To predict the tensile failure behavior, this study developed a finite element homogenization model for corrugated sandwich core plate structures. VUMAT and UGENS user programs were built to implement the Chow-Wang behavior model and the homogenization model in Abaqus software. The accuracy of the model was confirmed by comparing the results of the 3D model and the equivalent 2D model. The proposed model saves computational time and reduces the time for preparing geometric models, thereby reducing the cost in the design of corrugated sandwich core plates. In addition, the model also proves to be effective by being used as an alternative to 3D models in studying the stress-strain changes in tensile structures.

Author Statements:

- **Ethical approval:** The conducted research is not related to either human or animal use.
- **Conflict of interest:** The authors declare that they have no known competing financial interests or personal relationships that could have appeared to influence the work reported in this paper
- **Acknowledgement:** This research is supported by the Thai Nguyen University of Technology
- **Author contributions:** The authors declare that they have equal right on this paper.
- **Funding information:** The authors declare that there is no funding to be acknowledged.
- **Data availability statement:** The data that support the findings of this study are available on request from the corresponding author. The data are not publicly available due to privacy or ethical restrictions.

References

[1] M. R. M. Rejab, & W. J. Cantwell (2013). The mechanical behaviour of corrugated-core sandwich panels. *Composite Part B: Engineering, 47*, 267–277. https://doi.org/10.1016/j.compositesb.2012.10.031

[2] F. Xia, Y. Durandet, P. J. Tan, & D. Ruan (2022). Three-point bending performance of sandwich panels with various types of cores. *Thin-Walled Structures, 179*. https://doi.org/10.1016/j.tws.2022.109723

[3] J. Kortenoeven, B. Boon, & A. De Bruijn (2008). Application of sandwich panels in design and building of dredging ships. *Journal of Ship Production, 24*(3), 125–134. https://doi.org/10.5957/jsp.2008.24.3.125

[4] K. Ciesielczyk, & R. Studziński (2022). Experimental investigation of sandwich panels supported by thin-walled beams under various load arrangements and number of connectors. *Archives*

of Civil Engineering, *68*(4), 389–402. https://doi.org/10.24425/ace.2022.143045

[5] S. A. A. Khalkhali, N. Nariman-zadeh, & Sh. Khakshournia (2014). Optimal design of sandwich panels using multi-objective genetic algorithm and finite element method. *International Journal of Engineering*, *27*(3C). https://doi.org/10.5829/idosi.ije.2014.27.03c.06

[6] D. Bensahal, & M. N. Amrane (2016). Effects of material and geometrical parameters on the free vibration of sandwich beams. *International Journal of Engineering Transactions B: Applications*, *29*(2), 222–228. https://doi.org/10.5829/idosi.ije.2016.29.02b.11

[7] D. Muniraj, & V. M. Sreehari (2021). Experimental damage evaluation of honeycomb sandwich with composite face sheets under impact load. *International Journal of Engineering Transactions A: Basics*, *34*(4), 999–1007. https://doi.org/10.5829/ije.2021.34.04a.26

[8] F. Xia, P. J. Tan, & D. Ruan (2022). Failure mechanisms of corrugated sandwich panels under transverse three-point bending. *Journal of Sandwich Structures & Materials*, *24*(4), 1808–1827. https://doi.org/10.1177/10996362221086517

[9] A. Stefan, G. Pelin, C. E. Pelin, A. R. Petre, & M. Marin (2021). Manufacturing process, mechanical behavior and modeling of composite-structure sandwich panels. *INCAS Bulletin*, *13*(1), 183–191. https://doi.org/10.13111/2066-8201.2021.13.1.19

[10] L. Ke, K. Liu, G. Wu, Z. Wang, & P. Wang (2021). Multi-objective optimization design of corrugated steel sandwich panel for impact resistance. *Metals*, *11*(9). https://doi.org/10.3390/met11091378

[11] H. Abedzade Atar, M. Zarrebini, H. Hasani, & J. Rezaeepazhand (2021). Determination of corrugated core sandwich panels elastic constant based on three different experimental methods and effect of structural integrity on flexural properties. *SN Applied Sciences*, *3*(4). https://doi.org/10.1007/s42452-021-04424-8

[12] M. R. Schultz, L. Oremont, J. C. Guzman, D. McCarville, C. A. Rose, & M. W. Hilburger (2011). Compression behavior of fluted-core composite panels. In *Collection of Technical Papers – AIAA/ASME/ASCE/AHS/ASC Structures, Structural Dynamics and Materials Conference*. https://doi.org/10.2514/6.2011-2170

[13] F. Xia, T. Pang, G. Sun, & D. Ruan (2022). Longitudinal bending of corrugated sandwich panels with cores of various shapes. *Thin-Walled Structures*, *173*. https://doi.org/10.1016/j.tws.2022.109001

[14] N. Talbi, A. Batti, R. Ayad, & Y. Q. Guo (2009). An analytical homogenization model for finite element modelling of corrugated cardboard. *Composite Structures*, *88*(2), 280–289. https://doi.org/10.1016/j.compstruct.2008.04.008

[15] A. Batti (2009). Modèle d'homogénéisation analytique et analyse non linéaire des structures d'emballage en carton ondulé (Unpublished doctoral dissertation). Université de Reims Champagne-Ardenne.

[16] P. Duong, B. Abbès, Y. M. Li, A. D. Hammou, M. Makhlouf, & Y. Q. Guo (2013). An analytic homogenisation model for shear–torsion coupling problems of double corrugated core sandwich plates. *Journal of Composite Materials*, *47*(11), 1327–134. https://doi.org/10.1177/0021998312447206

[17] Z. Aboura, N. Talbi, S. Allaoui, & M. L. Benzeggagh (2004). Elastic behavior of corrugated cardboard: Experiments and modeling. *Composite Structures*, *63*(1), 53–62. https://doi.org/10.1016/S0263-8223(03)00131-4

[18] N. Buannic, P. Cartraud, & T. Quesnel (2003). Homogenization of corrugated core sandwich panels. *Composite Structures*, *59*(3), 299–312. https://doi.org/10.1016/S0263-8223(02)00246-5

[19] N. Stenberg, C. Fellers, & S. Östlund (2001). Plasticity in the thickness direction of paperboard under combined shear and normal loading. *Journal of Engineering Materials and Technology*, *123*(2), 184–190. https://doi.org/10.1115/1.1352747

[20] Y. Q. G. A. D. Hammou, P. T. M. Duong, B. Abbès, & M. Makhlouf (2012). Finite element simulation with a homogenization model: Cardboard packaging. *Mechanics & Industry*, *13*(3), 175–184.

[21] V. D. Luong et al. (2018). Finite element simulation of the strength of corrugated board boxes under impact dynamics. In *Lecture Notes in Mechanical Engineering, Part F3*, 369–380. https://doi.org/10.1007/978-981-10-7149-2_25

[22] V. D. Luong, F. Abbès, M. P. Hoang, P. T. M. Duong, & B. Abbès (2021). Finite element elastoplastic homogenization model of a corrugated-core sandwich structure. *Steel and Composite Structures*, *41*(3), 437–445. https://doi.org/10.12989/scs.2021.41.3.437

[23] V. D. Luong, A. S. Bonnin, F. Abbès, J. B. Nolot, D. Erre, & B. Abbès (2021). Finite element and experimental investigation on the effect of repetitive shock in corrugated cardboard packaging. *Journal of Applied and Computational Mechanics*, *7*(2), 820–830. https://doi.org/10.22055/jacm.2020.35968.2771

[24] D. L. Tien, N. T. T. Phuong, D. P. T. Minh, & V. D. Luong (2023). Finite element simulation for the plastic behavior of corrugated core sandwich panel. *Journal of the Serbian Society for Computational Mechanics*, *17*(2), 142–152. https://doi.org/10.24874/jsscm.2023.17.02.10

[25] D. L. Lien Tien Dao & P. T. M. Minh Duong (2024). Analysis of stress and strain in sandwich structures using an equivalent finite element model. *International Journal of Engineering and Technology Innovation*. https://doi.org/10.46604/ijeti.2024

[26] D. Mrówczyński & T. Garbowski (2023). Influence of imperfections on the effective stiffness of multilayer corrugated board. *Materials*, *16*(3). https://doi.org/10.3390/ma16031295

[27] C. L. Chow & J. Wang (1987). An anisotropic theory of continuum damage mechanics for ductile

fracture. *Engineering Fracture Mechanics*, *27*(5), 547–558. https://doi.org/10.1016/0013-7944(87)90108-1

[28] H. Lee, K. Peng, & J. Wang (1985). An anisotropic damage criterion for deformation instability and its application to forming limit analysis of metal plates. *Engineering Fracture Mechanics*, *21*, 1031–1054.

[29] J. N. Reddy (2003). *Mechanics of laminated composite plates and shells*. CRC Press. https://doi.org/10.1201/b12409

[30] N. Stenberg (2003). A model for the through-thickness elastic-plastic behaviour of paper. *International Journal of Solids and Structures*, *40*(26), 7483–7498. https://doi.org/10.1016/j.ijsolstr.2003.09.003

[31] D. Lien Tien Dao & V. D. Luong (2024). Inverse identification method of plasticity parameters of anisotropic material. *Journal of the Serbian Society for Computational Mechanics*, *18*(2), 106–119. https://doi.org/10.24874/jsscm.2024.18.02.07